

Eric A. D'Asaro<sup>1,2</sup>

<sup>2</sup>School of Oceanography, University of Washington, Seattle, WA

- Emerging observations, modeling and theory indicate that mixing in the ocean interior is usually not directly due to breaking internal waves
- Instead internal waves create patches of layered stratified turbulence that breaks to create 3D turbulence by shear instability
- Mixing efficiency is thus set by the properties of the layered stratified turbulence, not the internal waves

–1–

## Abstract

Mixing in the ocean interior clearly draws its energy from the internal wave field. The pathway is often described as “Internal wave breaking”, contrary to the observation that the smallest vertical internal wave scales are larger than the largest turbulence scales. Evidence for a different pathway is reviewed here: Internal waves generate patches of LAST, “layered stratified turbulence”, a well-characterized class of motions distinct from internal waves and three-dimensional turbulence. LAST dominates the dynamics in the  $10^1$ – $10^2$  range of vertical wavenumbers between internal waves and turbulence. It is possibly generated at transient critical layers, cascades energy to smaller scales and dissipates by generating patches of turbulence and mixing through shear instability. The existence of such patches is well-documented and the limited data suggests that they produce most of the mixing. The mixing efficiency is set by the properties of LAST, not the properties of internal waves.

## Plain Language Summary

The mixing of temperature and salinity in the ocean is an important part of the overall ocean circulation. Waves within the ocean generated at the surface and bottom are believed to cause this mixing although the exact mechanisms by which this occurs have not been well characterized. Here, a new pathway is suggested: The mixing is not caused directly by the breakdown of these waves as is commonly thought. Instead, the waves create a new type of oceanic motion consisting of thin flat pancake eddies and these eddies breakdown to cause the mixing.

## 1 Introduction

A recent book on ocean mixing (Garabato & Meredith, 2022) places the study of ocean mixing at a watershed. It is becoming a mature field, with well-established knowledge gained from decades of study, well poised to integrate this knowledge with the wider study of the oceans and earth. Nevertheless, some foundational issues still remain. One is reviewed here: The relationship between internal waves and mixing.

Our understanding of the sequence of processes that produce diapycnal mixing in the ocean interior has been broadly stable since the mid-1990s (D’Asaro, 1991). Internal waves are generated by wind at the surface and by the barotropic tide working on rough topography. These mostly generate low mode tidal and inertial frequency waves which can propagate long distances and fill the ocean basins with internal waves. Thus internal waves exist at similar levels over most of the open ocean, a surprising result that dominated early research (Wunsch & Webb, 1979). Some waves are dissipated locally, so that significant hot spots also exist (Rudnick et al., 2003), as well as broad regions with lower levels. In all of these locations, wave-wave interactions move energy from the low modes to a spectrum of higher modes and constrain the frequency-wavenumber spectrum of the waves to a nearly universal shape, the Garrett-Munk spectrum (Müller et al., 1986). Most importantly, the rate of energy transfer from large to small scales by wave-wave interactions depends on the internal wave energy level (M. C. Gregg, 1989). If this rate of energy transfer is assumed to be the energy input to turbulence, and a mixing efficiency is assumed (M. C. Gregg et al., 2018), then the mixing rate can be calculated. Thus the time and space distribution of mixing can be related to the generation, propagation and dissipation of internal waves. This powerful result has dominated research for the last 30 years (MacKinnon et al., 2017; C. B. Whalen et al., 2020), leaving the issue of exactly how energy gets from the internal waves to the mixing unresolved. I address this issue here.

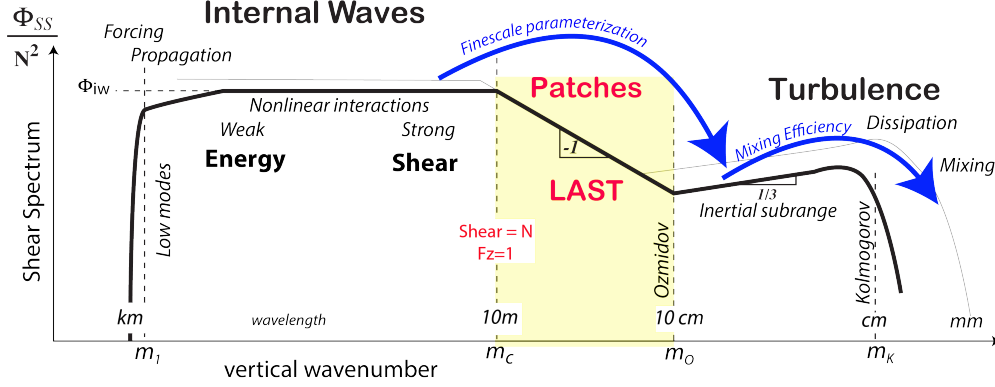


**Figure 1.** Scales and processes leading to diapycnal mixing in the ocean interior. Vertical wavelengths are appropriate for a roughly Garrett-Munk energy level. The change in spectral levels with higher internal wave energy is shown by the light gray lines. The blue arrows show parameterizations that allow energy flux from waves to turbulence to be calculated.

## 2 FineScale Parameterizations of mixing rate

Our understanding is often presented in terms of vertical wavenumber spectra. Figure 1 shows an idealized spectrum of the vertical wavenumber spectrum  $\Phi_{SS}(m)$  of the vertical shear, i.e. the average of the spectra of  $u_z$  and  $v_z$  where  $u$  and  $v$  are the horizontal velocity components and the subscript denotes the vertical  $z$  derivative. The spectra are scaled by the buoyancy frequency  $N$ , most strictly in a WKB-sense, although this is unimportant here. The scaled (or unscaled) spectra span a range of about  $10^6$  in scale, from wavelength of the lowest modes, to the mm scales of molecular diffusion. The shape and scalings are based on measurements across this entire range (M. Gregg et al., 1993; Gargett et al., 1981), although only occasionally at the same time and place. It thus broadly summarizes many decades of open ocean observations.

Starting on the left of Figure 1, wind and tides flux energy into the lowest few modes, with a lowest wavenumber of  $m_1$ . These waves are only weakly nonlinear so they can be dramatically more energetic near sources and can propagate long distances away from their sources. The shorter waves have stronger nonlinear interactions, resulting in a shear spectrum  $\Phi_{SS}(m)$  that is close to white, as described in the Garrett-Munk spectrum. Thus, the energy is concentrated in the low modes and the shear is concentrated in the shorter waves. Wave-wave interaction theory scales the rate at which energy is fluxed toward the shorter waves with the level of the shear spectrum squared. D’Asaro and Lien (2000) summarize these parameterizations as

$$\varepsilon = \frac{I_0}{Fr_c^2} N^2 f \Phi_{iw}^2, \quad (1)$$

where  $I_0 = 0.15$  combines various arbitrary “GM” scales, assumed energy ratios and spectral reflection coefficients,  $f$  is the Coriolis frequency and  $\Phi_{iw}$  is the level of the unscaled shear spectrum. The smallest internal waves have a wavenumber  $m_c$  such that the Froude function

$$\mathcal{F}(m_c) = \int_{m_1}^{m_c} \frac{\Phi_{SS}(m)}{N^2} dm = Fr_c \quad (2)$$

equals a critical value  $Fr_c$  of approximately 1. With this assumption, the shear due to internal waves is about  $N$ , or equivalently, the Richardson number due to internal waves is about 1. The energy flux  $\varepsilon$  toward small scales due to wave-wave interactions is thus computed from (1) using values of  $\Phi_{iw}$  near  $m_c$  as described in more detail by Polzin et al. (2014).

At vertical wavenumbers larger than  $m_c$ , the shear spectrum decreases with a slope of about -1 (Gargett et al., 1981) until a wavenumber of about  $m_O = 1/L_O$ , the Ozmidov wavenumber, where  $L_O = (\varepsilon/N^3)^{1/2}$  is the Ozmidov length. This is the largest scale of three dimensional turbulence and similar to the overturning (“Thorpe”) scale (S. A. Thorpe, 1977; Dillon, 1982; Smyth et al., 2001). Higher wavenumbers have an inertial subrange spectrum with a slope of +1/3 from approximately  $m_O$  to the Kolomogov wavenumber  $m_K$ . Mixing of temperature and salinity driven by this turbulence occur at even smaller scales, the Batchelor scale (Batchelor, 1959; Nash & Moum, 2002). The rate of mixing can be computed from the diapycnal diffusivity

$$K_\rho = \gamma\varepsilon/N^2 \quad (3)$$

(Osborn, 1980), where  $\gamma$  is the ‘mixing coefficient’, one of several possible varieties of mixing efficiencies (M. C. Gregg et al., 2018).

“Finescale Parameterizations” (Polzin et al., 2014) combine variants of (1) and (2) to compute  $\varepsilon$ . Values of  $\gamma$  are then assumed and (3) used to compute  $K_\rho$ . The combination derives mixing rates at cm and mm scales from measurements of internal wave properties at 10’s of meter scales. Variants of this approach (Kunze et al., 2006) use density profiles, rather than shear to estimate  $\varepsilon$  and have thus been able to compute diapycnal diffusivities from the millions of such profiles made from ships and profiling floats, thereby producing global maps of  $K_\rho$  (C. Whalen et al., 2012).

Such success and wide usage prompts a careful reexamination of the assumptions of this method. As sketched in Figure 1, the finescale parameterization and mixing efficiency assumptions jump over at least 3 orders of magnitude in scale, likely oversimplifying the physics of multiple processes. In particular, a recent vigorous debate about appropriate values of the mixing efficiency is summarized in M. C. Gregg et al. (2018) as “[S]ubstantial disagreements remain about mixing efficiency and coefficients, with estimates varying up to fivefold... A community effort is needed to focus observational, laboratory, and numerical approaches to mixing efficiency and mixing coefficients. To focus laboratory and numerical studies on relevant mechanisms and intensities, endeavors should begin with determining the mechanisms producing mixing in the ocean.”

### 3 Turbulent Patches

Turbulence in the ocean pycnocline is not randomly distributed but occurs in patches of high and low energy as shown in Figure 2. These are not explained by the standard models of ocean mixing, e.g. Figure 1, but may have an important role in mixing processes. Studies of turbulent patches have been limited, and mostly date from several decades ago. Based on this limited data, typical properties of turbulent patches are:

1. “Most mixing does not occur as isolated ... instabilities, but is formed in mixing zones containing many localized instabilities” (M. C. Gregg, 1984) .
2. Typical scales are 1-10m vertically and 50m-10km horizontally with an aspect ratio of about 1:100 (Rosenblum & Marmorino, 1990).
3. Patch scales are much larger than turbulent overturning scales. For example for the data in Figure 2, the Ozmidov scale is less than 20cm.
4. The patches are associated with near-inertial velocity features, as seen near 50m and 180m in Figure 2 and in Marmorino et al. (1987). Statistically, the strongest patches occur with the lowest Richardson numbers (Mack & Schoeberlein, 2004).

Patches are smaller than the internal wave scales and larger than the Ozmidov scale and thus exist within the ‘-1’ vertical wavenumber band. Thus, the spectral properties

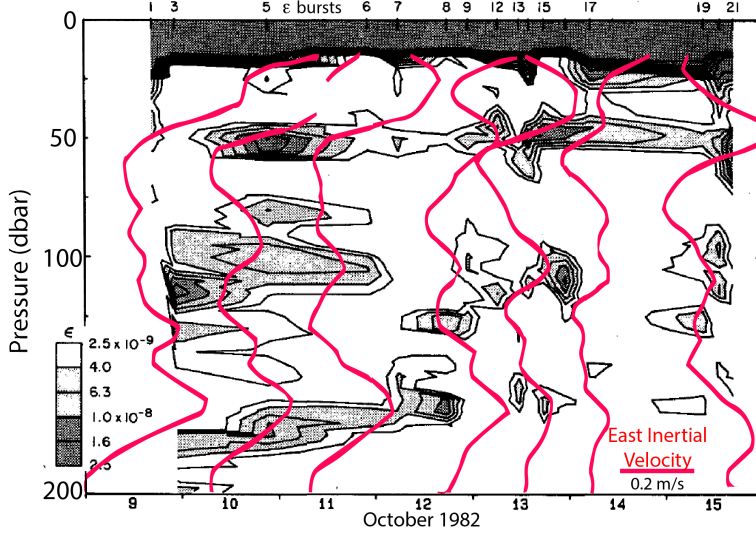


**Figure 2.** Turbulent patches measured using from microstructure profiles following a drogued buoy. Contours and shading show dissipation rate for a set of profile bursts, each containing 3-20 profiles and averaged to uniform 0.5 m bins. Red lines show one component of the inertial velocity computed from XCP velocity profiles every 1/4 inertial period. Figure modified from (M. C. Gregg et al., 1986).

of this range will be added to the list and the name *Patch Scales* used as a more descriptive synonym.

5. The vertical wavenumber shear spectrum has a slope is -1. As the energy flux  $\varepsilon$  increases, the spectra evolve as shown by the light gray line in Figure 1. The internal wave spectral level increases and the turbulence spectral level increases more, as specified by (1). However, the spectral level of the patch scale remains unchanged, although its endpoints  $m_c$  and  $m_O$  move to lower wavenumber and the shear variance between them increases. There is considerable experimental support for this result, with very similar scaled spectral levels found both in the ocean (Gargett et al., 1981; M. Gregg et al., 1993; Winkel, 1998) and in the middle atmosphere (Smith et al., 1987; Fritts, 1989; Allen & Vincent, 1995).
6. A similar spectrum is found for density fluctuations, but is not discussed here (M. C. Gregg, 1987).

Measurements by Klymak and Moum (2007) provide a crucial key to understanding the dynamics of the patch scales. Horizontal tows near Hawaii measured horizontal wavenumber spectra of the slope of isotherms and dissipation rate across a broad range of internal wave and mixing intensities (Figure 3). The spectra are fit accurately using the same model used to fit vertical wavenumber spectra: the sum of an inertial subrange with a slope of +1/3 and a small correction for the inertial-diffusive subrange at high wavenumber.

$$\Phi_{\zeta_x}(\alpha) = \chi_{\zeta} [C_T \varepsilon^{-\frac{1}{3}} \alpha^{\frac{1}{3}} + q \nu^{-\frac{1}{2}} \varepsilon^{-\frac{1}{2}} \alpha] \quad (4)$$

where  $\alpha = 2\pi k_x$  is the wavenumber in rad/m;  $\nu$  is the viscosity and  $C_T$  and  $q$  are empirical constants. The spectral shape, inside the brackets, is set only by  $\varepsilon$ ; the spectral level is set by  $\chi_{\zeta}$ . For vertical wavenumber spectra standard microstructure methods interpret  $\chi_{\zeta}$  as the dissipation rates of temperature variance scaled by the mean vertical

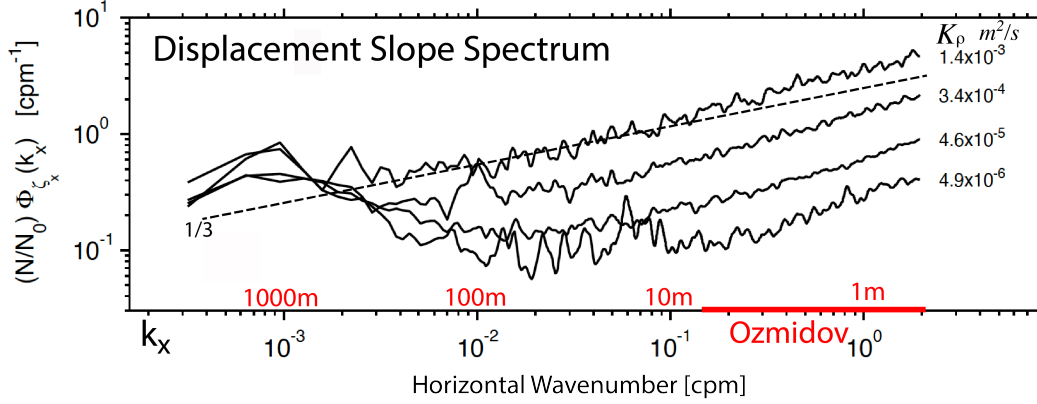


**Figure 3.** Horizontal wavenumber spectra of isopycnal slope near Hawaii for 4 regions with varying diapycnal diffusivities  $K_\rho$  computed from (3) rates. Red line has a slope of  $+1/3$ . Annotation on bottom axis indicates wavelength and range of Ozmidov wavenumbers. Figure modified from Klymak and Moum (2007).

gradient and  $\varepsilon$  as the dissipation rate of energy. However, for three-dimensional turbulence, this only applies for scales less than the Ozmidov scale. These observations, show the same spectral forms at scales 10 to 100 times larger. This suggests a similar turbulent cascade of both temperature and energy to small scales but carried by dominantly horizontal motions. This flow is therefore highly anisotropic and not standard 3D turbulence.

#### 4 Layered Stratified Turbulence

These properties of the patch scales do not match those of either internal waves or three-dimensional turbulence and thus defied interpretation from many years. Since the early days of internal wave research, the presence of significant velocity and density signatures that are inconsistent with internal wave dynamics has been apparent (Müller et al., 1978). These were often explained by the presence of a 'vortical mode' (Müller et al., 1986), different from internal waves because of its large potential vorticity component and different from 3-D turbulence because of its large anisotropy. However, this was not usually evoked as an explanation of the '-1' spectral regime.

Riley and Lindborg (2008) argue that the patch scales are dominated by a well-defined class of motions that are neither internal waves or 3-D turbulence. Falder et al. (2016) suggest the name LAST ("Layered Stratified Turbulence") to discriminate this from 3-D turbulence modified by stratification. Phenomenologically, consider the wake of a body towed through a stratified fluid (Lin & Pao, 1979) as described in Riley and Lelong (2000): "the near-field wake, in which  $[Fr]$  was rather large, remained approximately the same as in ... nonstratified experiments. In the far field, as the wake turbulence decayed,  $[Fr]$  became small and buoyancy forces became dominant, and the behavior of the wake changed dramatically. The wake appeared to consist of quasi-horizontal motions, reminiscent of a two-dimensional wake, but undulating in a sea of internal waves. These quasi horizontal motions appeared to have considerable vertical structure." In short, strong forcing excited a combination of 3D turbulence that decayed, internal waves that propagated into the entire domain, and LAST that became most prominent as the waves and turbulence decayed.

LAST has been the subject of numerous theoretical and numerical studies in the last decade (Billant & Chomaz, 2001; Bartello & Tobias, 2013; Portwood et al., 2016; Maffioli et al., 2016; Maffioli & Davidson, 2016; Maffioli, 2017; Howland et al., 2021; Chini et al., 2022). These have clearly defined its major properties. It occurs in the limit of high Reynolds number, small horizontal Froude number:

$$Fr \equiv U/NL \ll 1 \quad (5)$$

and small aspect ratio

$$Z/L \ll 1 \quad (6)$$

where  $U$ ,  $L$ ,  $h$ , and  $N$  are typical scales for horizontal velocity, horizontal scale, vertical scale and vertical density stratification, respectively. Under these conditions (Billant & Chomaz, 2001) the flow adjusts so that the vertical Froude number

$$F_z \equiv U/NZ \approx 1, \quad (7)$$

are much larger than the Ozmidov scale,

$$Z \gg L_O. \quad (8)$$

The horizontal momentum balance is primarily advective, and energy cascades to small scales at a rate

$$\varepsilon \approx U^3/L. \quad (9)$$

Following standard cascade arguments from 3D turbulence, the horizontal wavenumber spectra of velocity and density should have a -5/3 spectral slope; this is found in simulations (Maffioli, 2017). Despite the large aspect ratio, vertical velocities in LAST are strong enough to play an important dynamical role; the flow is not two-dimensional and a forward energy cascade, not inverse, cascade occurs. Furthermore, (7) implies that the vertical wavenumber spectrum of shear should scale as

$$\Phi_{U_z} \approx N^2/k_z \quad (10)$$

independent of  $\varepsilon$ . Kunze (2019) argues that the aspect ratio is limited by rotation so that

$$Z/L > f/N \quad (11)$$

These properties fit those observed for the Patch Scales in Section 2 above, implying that the Patch Scales are dominated by LAST. This argument is supported by the more detailed review of the observations and their synthesis into a model of spectral shapes by Kunze (2019) and the more detailed measurements of these by Vladoiu et al. (2022).

## 5 Generation of LAST

As in Figure 1, we expect that the energy cascade from internal waves to 3D turbulence passes through the Patch Scales. If these are mostly LAST, then LAST must be generated by internal waves with vertical wavenumbers near  $m_c$ . However, for internal waves vorticity is dominantly horizontal, aligned with isopycnals, so the Ertel potential vorticity (PV) is small, zero in simple linear waves. For LAST, the vorticity is dominantly vertical, perpendicular to isopycnals, so Ertel potential vorticity anomalies are large. The creation of LAST from internal waves therefore requires the creation of PV anomalies.

Finescale parameterizations are based on models of wave/wave interaction. A dominant class of these interactions is “induced diffusion” (Müller et al., 1986; Polzin et al., 2014) which can be represented as the refraction of small waves in a larger scale shear. The larger waves are only weakly nonlinear and can be modeled by weak wave-wave interaction theory (McComas & Müller, 1981); for smaller, more nonlinear waves, eikonal

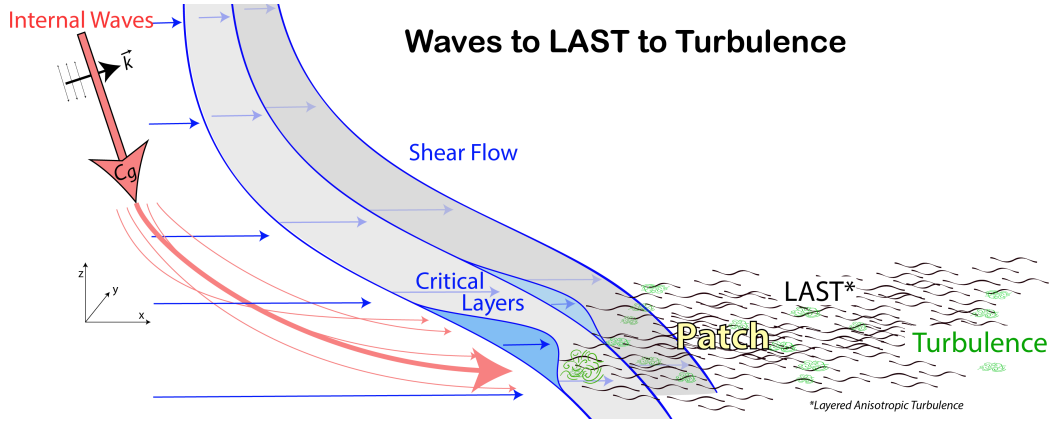


**Figure 4.** Cartoon of the proposed path from waves to turbulence in the ocean. A spectrum of small scale internal waves propagating in the shear of larger waves encounter three-dimensional critical layers where they stall, dissipate and transfer their energy to a patch of Layered Stratified Turbulence (LAST). The LAST cascades the energy to smaller scales, creating three-dimensional turbulence and mixing through shear instability.

or ray-tracing methods can be used (Heney, 1991; Heney et al., 1986). Although both yield predictions with similar scalings, the eikonal model is more appropriate for the smaller scales on which finescale parameterizations are applicable. Test waves are propagated through a background shear flow of other waves using ray theory. Their vertical wavenumber changes as they propagate. If the wavenumber becomes too large, the wave is assumed to dissipate to turbulence. The flux of energy to turbulence is taken as the sum of these individual dissipation events. This typically occurs close to a “critical layer” (Figure 4) where the horizontal phase speed  $c$  of the wave matches the background velocity,  $U(z_c) = c$ . As the wave approaches  $z_c$ , the vertical group velocity tends to zero and the energy density and shear grow indefinitely. For any particular set of waves, these layers are transient, changing in depth and location as the larger scale currents vary. For an ensemble of different waves, the different waves will have critical layers at different locations creating distinct patterns: (Heney, 1984): A typical critical level occurs at a “high-shear region is embedded in a much larger region with an average shear which is large and of the same sign as the smaller scale shear and ...not “shadowed” by a velocity peak...50-100 meters higher up...The critical layer has a large vertical extent – it is perhaps 20 meters thick.” Qualitatively, this matches properties #1, #2 and #4 of turbulent patches in Section 2 above, supporting the idea that patches occur at critical layers and that they are important.

The qualitative behavior of simple critical layers is well known. For small amplitude waves Booker and Bretherton (1967) show that as long as the Richardson number of the background shear is slightly larger than 0.25, almost all of the wave energy is transferred to the background flow, accelerating it in the direction of the wave propagation as sketched in Figure 4. Numerical and laboratory (S. Thorpe, 1981) simulations confirm this behavior, but show significant wave reflection for small Richardson number (Jones, 1968; Breeding, 1971). For finite amplitude waves, low resolution numerical simulations (Winters & D’Asaro, 1994) and laboratory studies (Dörnbrack, 1998) show instabilities near the critical layers that dissipate 20-30% of the unreflected wave energy with the remaining 70-80% of the wave energy accelerating the mean flow. Thus the primary effect of critical layers is to convert the energy of the waves to energy of the non-wave flow, mostly the mean kinetic energy, but also some turbulence.

To create LAST, much of the energy given up by the waves must be associated with PV anomalies. Bühler and McIntyre (2005) address this issue by noting that the non-linear advection by an isolated bounded internal wave packet, e.g. its Stokes drift, has a Lagrangian potential vorticity dipole aligned in the direction of propagation. Since without dissipation the potential vorticity of the fluid cannot change, a propagating packet must be accompanied by an Eulerian vortex dipole that cancels the packet's PV. When the wave dissipates, the Eulerian vortex remains, creating PV anomalies. This physics is not captured by the classical critical layer calculations and simulations, because the 2D wave packets considered in these have no lateral variability and thus no Lagrangian PV. The Booker and Bretherton (1967) calculation, for example, has zero PV throughput. In Winters and D'Asaro (1994), the flow is initially zero PV; only about 20-30% of the energy ends up in PV modes, mostly through the instabilities. Robust generation of LAST requires that most of the wave energy be transferred to PV modes. For this to occur, three-dimensional wave packets with gradients in directions perpendicular to the propagation direction and therefore capable of carrying PV need to be modeled.

## 6 A New Path to Turbulence?

### 6.1 Hypotheses

Figure 4 summarizes a new proposed path from internal waves to mixing. As in the current synthesis, low-mode internal waves generated by wind and tide generate a broad spectrum of waves via wave-wave interactions. The following hypotheses describe the subsequent path from the waves to turbulence:

- A: Small scale internal waves break down into patches of turbulence and Layered Anisotropic Turbulence (LAST) at transient critical layers associated with regions of large vertical internal wave and/or geostrophic shear. The size and location of these patches are set by the dynamics of the critical layers.
- B: Energy is transferred from the internal wave scales to turbulence by LAST. The properties of the scales between internal waves and turbulence, the 'Patch Scales', are set by the dynamics of LAST within the patches.
- C: LAST generates turbulence through shear instability near the Ozmidov scale. The properties of the turbulence, including the mixing efficiency, are set by the details of these instabilities.

### 6.2 Discussion

Hypothesis B rests on strong evidence that the '-1' spectral regime is dominated by LAST. As described above and elaborated by Kunze (2019), the observed vertical and horizontal wavenumber spectra, their scalings, and the apparent quasi-horizontal energy cascade are consistent with LAST.

Hypothesis C seems likely given hypothesis B. Maffioli et al. (2016) simulates the mixing efficiency for LAST as a function of  $Fr$  finding a value of about 0.3 for the smallest values. However, the wide range of scales in oceanic LAST makes this a challenging numerical problem (Chini et al., 2022) that has yet to be fully addressed.

Hypothesis A is the most speculative. Hypothesis B clearly implies an energy transfer from internal waves to LAST. Kunze (2019) hypothesized an unspecified internal wave instability to accomplish this. Critical layers are presented here as a more concrete alternative. Nevertheless, we know little about the properties of turbulent patches, about the properties of the internal wave packets that are hypothesized to create these patches, or the detailed theory necessary to predict the patch properties from the wave proper-

ties. In particular, the mechanisms by which internal waves create the PV anomalies essential to LAST remain obscure. Both the three-dimensionality of the internal wave packets and the dissipative effects of turbulence appear to play a crucial role.

## 7 Implications

This review summarizes and elaborates on several decades of research indicating that internal wave breaking does not directly cause turbulence in the ocean interior. Instead, the internal waves create LAST, and LAST creates turbulence. This has little impact on the utility of finescale parameterizations to estimate the energy transfer from internal waves to mixing. However, by focusing studies of oceanic mixing efficiency on LAST instead of on internal waves it may help the ocean mixing community converge on mixing efficiency estimates that are appropriate for the real ocean, as recommended by M. C. Gregg et al. (2018).

Dye observations consistently show a small-scale along-isopycnal diffusivity of roughly  $1m^2s^{-1}$  in the ocean interior more, than can be explained by shear dispersion (Sundermeyer et al., 2020). Explanations have included nonlinear internal wave transport (Bühler et al., 2013) and PV generation by diapycnal mixing events and weak wave/wave/vortex interaction (Sundermeyer & Lelong, 2005). LAST is intrinsically dispersive in the horizontal as it is both vortical and dissipative. The work reviewed here suggests that this lateral dispersion is intimately connected with diapycnal dispersion: both are supported by the energy cascade  $\varepsilon$  from waves to turbulence. LAST is responsible for the lateral dispersion, perhaps with the traditional dispersion rate proportional to  $(\varepsilon L^4)^{1/3}$ ; turbulence is responsible the diapycnal dispersion at a rate proportional to  $\varepsilon/N^2$  (3). This very different scaling with  $\varepsilon$  and  $N$  can perhaps provide a test of this hypothesis.

The canonical spectrum of shear in the ocean interior (Figure 1) shows a mixture of internal waves, LAST and turbulence. D’Asaro and Lien (2000) show that this breaks down for sufficiently strong forcing. As the internal wave energy increases,  $m_c$  decreases until the bandwidth of the internal wave regime,  $m_c - m_1$  goes to zero. This occurs when  $F_z$  (7) becomes order one. D’Asaro and Lien (2000) show data indicating that although the internal wave regime disappears, the “-1” region remains. In this case, the forcing directly creates LAST. D’Asaro and Lien (2000) call this the “Wave-Turbulence Transition”, but it should be more properly called the “LAST-Wave Transition.” At lower energies,  $\varepsilon$  varies as energy squared, as in (1); at higher energies  $\varepsilon$  varies linearly with energy. The observations by Bouruet-Aubertot et al. (2010) of a linear relationship between dissipation and energy level in the strongly forced flows in Rockall Channel support this idea. More generally, the recognition that LAST is a distinct and important mode of oceanic motion, worthy of much additional study, is likely to result in finding it frequently in a wide range of environments.

## 8 Open Research

No data was used in this manuscript.

## Acknowledgments

I thank Eric Kunze for stimulating discussions on this topic over many years, the 2022 Gordon Research Conference on Ocean Mixing for making me think about it, and Leif Thomas and Raffaele Ferrari for pointing me in fruitful theoretical directions. I apologize to the authors of many fine papers on this topic that I have neglected in this review. This work was funded by NSF grant OCE-1657676.

## References

- Allen, S. J., & Vincent, R. A. (1995). Gravity wave activity in the lower atmosphere: Seasonal and latitudinal variations. *Journal of Geophysical Research: Atmospheres*, 100(D1), 1327–1350. doi: <https://doi.org/10.1029/94JD02688>
- Bartello, P., & Tobias, S. (2013). Sensitivity of stratified turbulence to the buoyancy reynolds number. *Journal of Fluid Mechanics*, 725, 1–22. doi: <https://doi.org/10.1017/jfm.2013.170>
- Batchelor, G. K. (1959). Small-scale variation of convected quantities like temperature in turbulent fluid part 1. general discussion and the case of small conductivity. *Journal of fluid mechanics*, 5(1), 113–133. doi: <https://doi.org/10.1017/S002211205900009X>
- Billant, P., & Chomaz, J.-M. (2001). Self-similarity of strongly stratified inviscid flows. *Physics of fluids*, 13(6), 1645–1651. doi: <https://doi.org/10.1063/1.1369125>
- Booker, J. R., & Bretherton, F. P. (1967). The critical layer for internal gravity waves in a shear flow. *Journal of fluid mechanics*, 27(3), 513–539. doi: <https://doi.org/10.1017/S0022112067000515>
- Bouruet-Aubertot, P., Van Haren, H., & Lelong, M. P. (2010). Stratified inertial subrange inferred from in situ measurements in the bottom boundary layer of the rockall channel. *Journal of physical oceanography*, 40(11), 2401–2417. doi: <https://doi.org/10.1175/2010JPO3957.1>
- Breeding, R. (1971). A non-linear investigation of critical levels for internal atmospheric gravity waves. *Journal of Fluid Mechanics*, 50(3), 545–563. doi: <https://doi.org/10.1017/S0022112071002751>
- Bühler, O., Grisouard, N., & Holmes-Cerfon, M. (2013). Strong particle dispersion by weakly dissipative random internal waves. *Journal of Fluid Mechanics*, 719. doi: <https://doi.org/10.1017/jfm.2013.71>
- Bühler, O., & McIntyre, M. E. (2005). Wave capture and wave–vortex duality. *Journal of Fluid Mechanics*, 534, 67–95. doi: <https://doi.org/10.1017/S0022112005004374>
- Chini, G. P., Michel, G., Julien, K., Rocha, C. B., & Colm-cille, P. C. (2022). Exploiting self-organized criticality in strongly stratified turbulence. *Journal of Fluid Mechanics*, 933. doi: <https://doi.org/10.1017/jfm.2021.1060>
- D’Asaro, E. A. (1991). A strategy for investigating and modeling internal wave sources and sinks. In *Dynamics of oceanic internal gravity waves ii: Proceedings of ‘aha huliko’a hawaiian winter workshop* (pp. 451–466). (Available at <http://www.soest.hawaii.edu/PubServices/AhaHulikoa.html>)
- D’Asaro, E. A., & Lien, R.-C. (2000). The wave–turbulence transition for stratified flows. *Journal of Physical Oceanography*, 30(7), 1669–1678. doi: [https://doi.org/10.1175/1520-0485\(2000\)030<1669:TWTTF>2.0.CO;2](https://doi.org/10.1175/1520-0485(2000)030<1669:TWTTF>2.0.CO;2)
- Dillon, T. M. (1982). Vertical overturns: A comparison of thorpe and ozmidov length scales. *Journal of Geophysical Research: Oceans*, 87(C12), 9601–9613. doi: <https://doi.org/10.4319/lo.1983.28.5.0801>
- Dörnbrack, A. (1998). Turbulent mixing by breaking gravity waves. *Journal of Fluid Mechanics*, 375, 113–141. doi: <https://doi.org/10.1017/S0022112098002833>
- Falder, M., White, N., & Caulfield, C. (2016). Seismic imaging of rapid onset of stratified turbulence in the south atlantic ocean. *Journal of Physical Oceanography*, 46(4), 1023–1044. doi: <https://doi.org/10.1175/JPO-D-15-0140.1>
- Fritts, D. C. (1989). A review of gravity wave saturation processes, effects, and variability in the middle atmosphere. *pure and applied geophysics*, 130(2), 343–371. doi: <https://doi.org/10.1007/BF00874464>
- Garabato, A. N., & Meredith, M. (2022). Ocean mixing: oceanography at a watershed. In *Ocean mixing* (pp. 1–4). Elsevier. doi: <https://doi.org/10.1016/B978-0-12-821512-8.00008-6>

- Gargett, A., Hendricks, P., Sanford, T., Osborn, T., & Williams, A. (1981). A composite spectrum of vertical shear in the upper ocean. *Journal of Physical Oceanography*, 11(9), 1258–1271. doi: [https://doi.org/10.1175/1520-0485\(1981\)011<1258:ACSOVS>2.0.CO;2](https://doi.org/10.1175/1520-0485(1981)011<1258:ACSOVS>2.0.CO;2)
- Gregg, M., Winkel, D., & Sanford, T. (1993). Varieties of fully resolved spectra of vertical shear. *Journal of physical oceanography*, 23(1), 124–141. doi: [https://doi.org/10.1175/1520-0485\(1993\)023<0124:VOFRSO>2.0.CO;2](https://doi.org/10.1175/1520-0485(1993)023<0124:VOFRSO>2.0.CO;2)
- Gregg, M. C. (1984). Persistent mixing and near-inertial waves. In *Internal waves and small-scale turbulence: Proceedings of 'aha huli'ko'a hawaiian winter workshop* (pp. 1–24). (Available at <https://apps.dtic.mil/sti/citations/ADA149510>)
- Gregg, M. C. (1987). Diapycnal mixing in the thermocline: A review. *Journal of Geophysical Research: Oceans*, 92(C5), 5249–5286. doi: <https://doi.org/10.1029/JC092iC05p05249>
- Gregg, M. C. (1989). Scaling turbulent dissipation in the thermocline. *Journal of Geophysical Research: Oceans*, 94(C7), 9686–9698. doi: <https://doi.org/10.1029/JC094iC07p0968>
- Gregg, M. C., D'Asaro, E., Shay, T., & Larson, N. (1986). Observations of persistent mixing and near-inertial internal waves. *Journal of Physical Oceanography*, 16(5), 856–885. doi: [https://doi.org/10.1175/1520-0485\(1986\)016%3C0856:OOPMAN%3E2.0.CO;2](https://doi.org/10.1175/1520-0485(1986)016%3C0856:OOPMAN%3E2.0.CO;2)
- Gregg, M. C., D'Asaro, E. A., Riley, J. J., & Kunze, E. (2018). Mixing efficiency in the ocean. *Annual review of marine science*, 10(1). doi: <https://doi.org/10.1146/annurev-marine-121916-063643>
- Heney, F. S. (1984). transport of small scale internal waves toward microstructure. In *Internal waves and small-scale turbulence: Proceedings of 'aha huli'ko'a hawaiian winter workshop* (pp. 201–219). (Available at <https://apps.dtic.mil/sti/citations/ADA149510>)
- Heney, F. S. (1991). Scaling internal wave predictions for dissipation. In *Dynamics of oceanic internal gravity waves ii: Proceedings of 'aha huli'ko'a hawaiian winter workshop* (p. 233-236). (Available at <http://www.soest.hawaii.edu/PubServices/AhaHulikoa.html>)
- Heney, F. S., Wright, J., & Flatté, S. M. (1986). Energy and action flow through the internal wave field: An eikonal approach. *Journal of Geophysical Research: Oceans*, 91(C7), 8487–8495. doi: <https://doi.org/10.1029/JC091iC07p08487>
- Howland, C. J., Taylor, J. R., & Caulfield, C. (2021). Shear-induced breaking of internal gravity waves. *Journal of fluid mechanics*, 921. doi: <https://doi.org/10.1017/jfm.2021.506>
- Jones, W. L. (1968). Reflexion and stability of waves in stably stratified fluids with shear flow: A numerical study. *Journal of Fluid Mechanics*, 34(3), 609–624. doi: <https://doi.org/10.1017/S0022112068002119>
- Klymak, J. M., & Moum, J. N. (2007). Oceanic isopycnal slope spectra. part ii: Turbulence. *Journal of physical oceanography*, 37(5), 1232–1245. doi: <https://doi.org/10.1175/JPO3074.1>
- Kunze, E. (2019). A unified model spectrum for anisotropic stratified and isotropic turbulence in the ocean and atmosphere. *Journal of Physical Oceanography*, 49(2), 385–407. doi: <https://doi.org/10.1175/JPO-D-18-0092.1>
- Kunze, E., Firing, E., Hummon, J. M., Chereskin, T. K., & Thurnherr, A. M. (2006). Global abyssal mixing inferred from lowered adcp shear and ctd strain profiles. *Journal of Physical Oceanography*, 36(8), 1553–1576. doi: <https://doi.org/10.1175/JPO2926.1>
- Lin, J.-T., & Pao, Y.-H. (1979). Wakes in stratified fluids. *Annual Review of Fluid Mechanics*, 11, 317–338. doi: [https://ui.adsabs.harvard.edu/link\\_gateway/1979AnRFM..11..317L/doi:10.1146/annurev.fl.11.010179.001533](https://ui.adsabs.harvard.edu/link_gateway/1979AnRFM..11..317L/doi:10.1146/annurev.fl.11.010179.001533)
- Mack, S., & Schoeberlein, H. (2004). Richardson number and ocean mix-

- ing: Towed chain observations. *Journal of physical oceanography*, 34(4), 736–754. doi: [https://doi.org/10.1175/1520-0485\(2004\)034%3C0736:RNAOMT%3E2.0.CO;2](https://doi.org/10.1175/1520-0485(2004)034%3C0736:RNAOMT%3E2.0.CO;2)
- MacKinnon, J. A., Zhao, Z., Whalen, C. B., Waterhouse, A. F., Trossman, D. S., Sun, O. M., ... others (2017). Climate process team on internal wave-driven ocean mixing. *Bulletin of the American Meteorological Society*, 98(11), 2429–2454. doi: <https://doi.org/10.1175/BAMS-D-16-0030.1>
- Maffioli, A. (2017). Vertical spectra of stratified turbulence at large horizontal scales. *Physical Review Fluids*, 2(10), 104802. doi: <https://doi.org/10.1103/PhysRevFluids.2.104802>
- Maffioli, A., Brethouwer, G., & Lindborg, E. (2016). Mixing efficiency in stratified turbulence. *Journal of Fluid Mechanics*, 794. doi: <https://doi.org/10.1017/jfm.2016.206>
- Maffioli, A., & Davidson, P. A. (2016). Dynamics of stratified turbulence decaying from a high buoyancy reynolds number. *Journal of Fluid Mechanics*, 786, 210–233. doi: <https://doi.org/10.1017/jfm.2015.667>
- Marmorino, G., Rosenblum, L., & Trump, C. (1987). Fine-scale temperature variability: The influence of near-inertial waves. *Journal of Geophysical Research: Oceans*, 92(C12), 13049–13062. doi: <https://doi.org/10.1029/JC092iC12p13049>
- McComas, C. H., & Müller, P. (1981). The dynamic balance of internal waves. *Journal of Physical Oceanography*, 11(7), 970–986. doi: [https://doi.org/10.1175/1520-0485\(1981\)011%3C0970:TDBOIW%3E2.0.CO;2](https://doi.org/10.1175/1520-0485(1981)011%3C0970:TDBOIW%3E2.0.CO;2)
- Müller, P., Holloway, G., Henyey, F., & Pomphrey, N. (1986). Nonlinear interactions among internal gravity waves. *Reviews of Geophysics*, 24(3), 493–536. doi: <https://doi.org/10.1029/RG024i003p00493>
- Müller, P., Olbers, D. J., & Willebrand, J. (1978). The iwex spectrum. *Journal of Geophysical Research: Oceans*, 83(C1), 479–500. doi: <https://doi.org/10.1029/JC083iC01p00479>
- Nash, J. D., & Moum, J. N. (2002). Microstructure estimates of turbulent salinity flux and the dissipation spectrum of salinity. *Journal of physical oceanography*, 32(8), 2312–2333. doi: [https://doi.org/10.1175/1520-0485\(2002\)032%3C2312:MEOTSF%3E2.0.CO;2](https://doi.org/10.1175/1520-0485(2002)032%3C2312:MEOTSF%3E2.0.CO;2)
- Osborn, T. (1980). Estimates of the local rate of vertical diffusion from dissipation measurements. *Journal of physical oceanography*, 10(1), 83–89. doi: [https://doi.org/10.1175/1520-0485\(1980\)010%3C0083:EOTLRO%3E2.0.CO;2](https://doi.org/10.1175/1520-0485(1980)010%3C0083:EOTLRO%3E2.0.CO;2)
- Polzin, K. L., Naveira Garabato, A. C., Huussen, T. N., Sloyan, B. M., & Waterman, S. (2014). Finescale parameterizations of turbulent dissipation. *Journal of Geophysical Research: Oceans*, 119(2), 1383–1419. doi: <https://doi.org/10.1002/2013JC008979>
- Portwood, G. D., de Bruyn Kops, S. M., Taylor, J. R., Salehipour, H., & Caulfield, C. (2016). Robust identification of dynamically distinct regions in stratified turbulence. *Journal of Fluid Mechanics*, 807. doi: <https://doi.org/10.1017/jfm.2016.617>
- Riley, J. J., & Lelong, M.-P. (2000). Fluid motions in the presence of strong stable stratification. *Annual review of fluid mechanics*, 32(1), 613–657. doi: <https://doi.org/10.1146/annurev.fluid.32.1.613>
- Riley, J. J., & Lindborg, E. (2008). Stratified turbulence: A possible interpretation of some geophysical turbulence measurements. *Journal of the Atmospheric Sciences*, 65(7), 2416–2424. doi: <https://doi.org/10.1175/2007JAS2455.1>
- Rosenblum, L., & Marmorino, G. (1990). Statistics of mixing patches observed in the sargasso sea. *Journal of Geophysical Research: Oceans*, 95(C4), 5349–5357. doi: <https://doi.org/10.1029/JC095iC04p05349>
- Rudnick, D. L., Boyd, T. J., Brainard, R. E., Carter, G. S., Egbert, G. D., Gregg, M. C., ... others (2003). From tides to mixing along the hawaiian ridge.

- 510 *science*, 301(5631), 355–357. doi: DOI:10.1126/science.1085837
- 511 Smith, S. A., Fritts, D. C., & Vanzandt, T. E. (1987). Evidence for a saturated  
512 spectrum of atmospheric gravity waves. *Journal of Atmospheric Sciences*,  
513 44(10), 1404–1410. doi: [https://doi.org/10.1175/1520-0469\(1987\)044%3C1404:](https://doi.org/10.1175/1520-0469(1987)044%3C1404:EFASSO%3E2.0.CO;2)  
514 [EFASSO%3E2.0.CO;2](https://doi.org/10.1175/1520-0469(1987)044%3C1404:EFASSO%3E2.0.CO;2)
- 515 Smyth, W., Moum, J., & Caldwell, D. (2001). The efficiency of mixing in tur-  
516 bulent patches: Inferences from direct simulations and microstructure ob-  
517 servations. *Journal of Physical Oceanography*, 31(8), 1969–1992. doi:  
518 [https://doi.org/10.1175/1520-0485\(2001\)031\(1969:TEOMIT\)2.0.CO;2](https://doi.org/10.1175/1520-0485(2001)031(1969:TEOMIT)2.0.CO;2)
- 519 Sundermeyer, M. A., Birch, D. A., Ledwell, J. R., Levine, M. D., Pierce, S. D., &  
520 Kuebel Cervantes, B. T. (2020). Dispersion in the open ocean seasonal pycn-  
521 ocline at scales of 1–10 km and 1–6 days. *Journal of Physical Oceanography*,  
522 50(2), 415–437. doi: <https://doi.org/10.1175/JPO-D-19-0019.1>
- 523 Sundermeyer, M. A., & Lelong, M.-P. (2005). Numerical simulations of lateral  
524 dispersion by the relaxation of diapycnal mixing events. *Journal of physical*  
525 *oceanography*, 35(12), 2368–2386. doi: <https://doi.org/10.1175/JPO2834.1>
- 526 Thorpe, S. (1981). An experimental study of critical layers. *Journal of Fluid Me-*  
527 *chanics*, 103, 321–344. doi: <https://doi.org/10.1017/S0022112081001365>
- 528 Thorpe, S. A. (1977). Turbulence and mixing in a scottish loch. *Philosophical Trans-*  
529 *actions of the Royal Society of London. Series A, Mathematical and Physical*  
530 *Sciences*, 286(1334), 125–181. doi: <https://doi.org/10.1098/rsta.1977.0112>
- 531 Vladoiu, A., Lien, R.-C., & Kunze, E. (2022). Two-dimensional wavenumber spec-  
532 tra on the horizontal submesoscale and vertical finescale. *Journal of Physical*  
533 *Oceanography*. doi: <https://doi.org/10.1175/JPO-D-21-0111.1>
- 534 Whalen, C., Talley, L., & MacKinnon, J. (2012). Spatial and temporal variability of  
535 global ocean mixing inferred from argo profiles. *Geophysical Research Letters*,  
536 39(18). doi: <https://doi.org/10.1029/2012GL053196>
- 537 Whalen, C. B., De Lavergne, C., Naveira Garabato, A. C., Klymak, J. M., Mackin-  
538 non, J. A., & Sheen, K. L. (2020). Internal wave-driven mixing: Governing  
539 processes and consequences for climate. *Nature Reviews Earth & Environment*,  
540 1(11), 606–621. doi: <https://doi.org/10.1038/s43017-020-0097-z>
- 541 Winkel, D. P. (1998). *Influences of mean shear in the florida current on turbu-*  
542 *lent production by internal waves*. University of Washington. (Available at  
543 [https://www.proquest.com/dissertations-theses/influences-mean-shear-florida-](https://www.proquest.com/dissertations-theses/influences-mean-shear-florida-current-on/docview/304462012/se-2?accountid=14784)  
544 [current-on/docview/304462012/se-2?accountid=14784](https://www.proquest.com/dissertations-theses/influences-mean-shear-florida-current-on/docview/304462012/se-2?accountid=14784))
- 545 Winters, K. B., & D’Asaro, E. A. (1994). Three-dimensional wave instability near a  
546 critical level. *Journal of Fluid Mechanics*, 272, 255–284. doi: <https://doi.org/10.1017/S0022112094004465>
- 547 Wunsch, C., & Webb, S. (1979). The climatology of deep ocean internal waves.  
548 *Journal of Physical Oceanography*, 9(2), 235–243. doi: [https://doi.org/10.1175/1520-0485\(1979\)009\(0235:TCODOI\)2.0.CO;2](https://doi.org/10.1175/1520-0485(1979)009(0235:TCODOI)2.0.CO;2)  
549  
550